A second advantage is that the variation in K-values found is considerably less than those found with small-scale methods. For example, El-Mowelhi and Van Schilfgaarde (1982) found the K-values determined from different 100 mm drains in a clay soil to vary from 0.086 to 0.12 m/d. This range compares very favourably with the much wider ranges given in Sections 12.5.3 and 12.5.4.

Influence of Drainage Conditions
The choice of the correct drainage formula for the calculation of K-values from observations on the functioning of the drains depends on:
- The drainage conditions and the aquifer type. For example, the choice depends on the depth of an impermeable layer, whether the K-value increases or decreases with depth, and whether the aquifer is semi-confined and seepage or natural drainage occurs;
- Whether one is dealing with parallel drains with overlapping zones of influence or with single drains;
- Whether one analyses the drain functioning in steady or unsteady state;
- Whether the groundwater flow is two-dimensional (which occurs when the recharge is evenly distributed over the area) or three-dimensional (which often occurs in irrigated areas where the fields are not irrigated at the same time, so that the recharge is not evenly distributed over the area);
- Whether the drains are offering entrance resistance to the flow of groundwater into the drains or not;
- Whether the drains are placed in flat or in sloping land, and whether they are laid at equal or different depths below the soil surface.

In this chapter, not all the above situations will be discussed in detail, but a selection is presented in Section 12.7. Some other situations are described by Oosterbaan (1990a, 1990b).

The analysis of the functioning of existing drains in unsteady-state conditions offers the additional possibility of determining the drainable porosity (e.g. El-Mowelhi and Van Schilfgaarde 1982). This possibility is not further elaborated in this chapter.

Anyone needing to analyze K-values under drainage conditions that deviate from those selected in this chapter and are not discussed elsewhere in literature, will probably have to develop a new method of analysis which takes into account the specific drainage conditions.

12.6 Examples of Small-Scale In-Situ Methods

12.6.1 The Auger-Hole Method

Principle
The principle of the auger-hole method is as follows. A hole is bored into the soil with an auger to a certain depth below the watertable. When the water in the hole reaches equilibrium with the groundwater, part of it is removed. The groundwater then begins to seep into the hole and the rate at which it rises is measured. The hydraulic conductivity of the soil is computed with a formula or graph describing the mutual

relationship between the rate of rise, the groundwater conditions, and the geometry of the hole.

This method measures the average hydraulic conductivity of a soil column about 30 cm in radius and extending from the watertable to about 20 cm below the bottom of the hole, or to a relatively impermeable layer if it occurs within 20 cm of the bottom.

The method can also be used to measure the K-values of two separate layers. This is done by repeating the measurements in the same hole after it has been deepened. Reference is made to Van Beers (1970).

Theory

As reported by Van Beers (1970) and Bouwer and Jackson (1974), Ernst developed the following equation for the K-value of the soil in dependence of the average rate of rise of the water level in the hole (Figure 12.13)

$$K = C\frac{H_0 - H_t}{t} \tag{12.9}$$

where

K = hydraulic conductivity of the saturated soil (m/d)
C = a factor as defined in Equation 12.10 or 12.11
t = time elapsed since the first measurement of the level of the rising water in the hole (s)

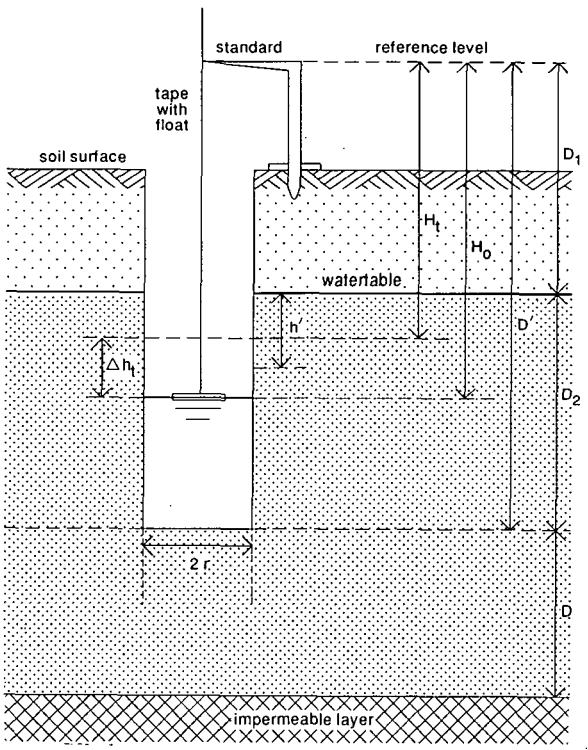

Figure 12.13 Measurements for the auger-hole method

H_t = depth of the water level in the hole below reference level at time t (cm)
H_o = H_t when t = 0

The C-factor depends on the depth of an impermeable layer below the bottom of the hole (D) and the average depth of the water level in the hole below the watertable (h′) as follows:

When $D > \frac{1}{2} D_2$, then

$$C = \frac{4000 \frac{r}{h'}}{\left(20 + \frac{D_2}{r}\right)\left(2 - \frac{h'}{D_2}\right)} \qquad (12.10)$$

When D = 0, then

$$C = \frac{3600 \frac{r}{h'}}{\left(10 + \frac{D_2}{r}\right)\left(2 - \frac{h'}{D_2}\right)} \qquad (12.11)$$

where

D = depth of the impermeable layer below the bottom of the hole (cm)
D_2 = depth of the bottom of the hole below the watertable (cm), with the condition: $20 < D_2 < 200$
r = radius of the hole (cm): $3 < r < 7$
h′ = average depth of the water level in the hole below the watertable (cm), with the condition: $h' > D_2/5$

When $0 < D < \frac{1}{2} D_2$, one must interpolate between the results of the above two equations.

The value of h′ can be calculated from

$$h' = 0.5 (H_0 + H_n) - D_1 \qquad (12.12)$$

where

D_1 = depth of the watertable below reference level (cm)
H_n = depth of the water level in the hole at the end of the measurements (cm)

Ernst also prepared graphs for the solution of the C-factor in Equation 12.9 (Van Beers 1970), which are more accurate than Equations 12.10 and 12.11. Within the ranges of r and H mentioned above, however, the equations give less than 20% error. In view of the usually large variability in K-values (of the order of 100 to 1000%, or more), the given equations are accurate enough.

Other methods of determining K-values with the auger-hole method were reviewed by Bouwer and Jackson (1974). These methods give practically the same results as the Ernst method.

Equipment and Procedure

The equipment used in The Netherlands is illustrated in Figure 12.14. It consists of a tube, 60 cm long, the bottom end of which is fitted with a clack valve so that it can be used as a bailer. Extension pieces can be screwed to the top end of the tube. A float, a light-weight steel tape, and a standard are also part of the equipment. The standard is pressed into the soil down to a certain mark, so that the water-level readings can be taken at a fixed height above the ground surface.

The hole must be made with a minimum disturbance to the soil. The open blade auger used in The Netherlands is very suitable for wet clay soils, whereas the closed pothole auger commonly used in the U.S.A. is excellent in dry soils.

The optimum depth of the holes depends on the nature, thickness, and sequence of soil layers, on the depth of the watertable, and on the depth at which one wishes to determine the hydraulic conductivity. When augering the hole in slowly permeable soils, one often observes that the water is entering the hole only when the depth of the hole is well below the watertable. As the hole is deepened further, the water enters faster, because the rate of inflow of the water is governed by the difference between the watertable and the water level in the hole, and by the depth of the hole below reference level (D_2). Sometimes, this phenomenon is incorrectly attributed to artesian pressure, but artesian pressure only exerts an influence if one pierces a completely or almost impermeable layer.

When the water in the hole is in equilibrium with the groundwater, the level is recorded. Water is then bailed out to lower the level in the hole by 20 to 40 cm.

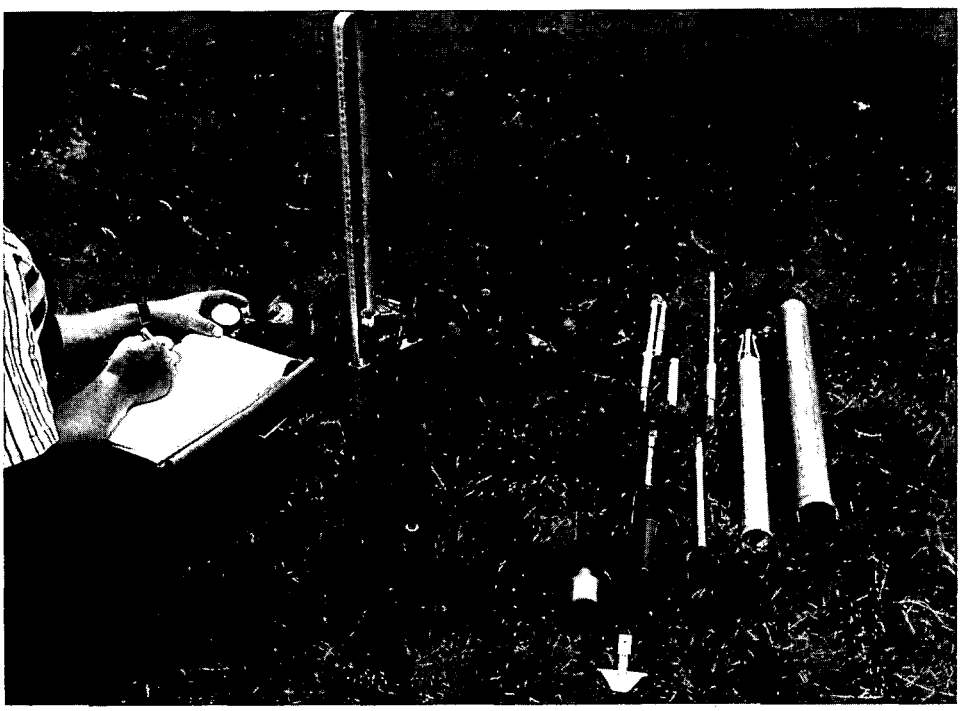

Figure 12.14 Equipment used for the auger-hole method (courtesy Eijkelkamp b.v.)

Measuring the rate of rise in the water level must begin immediately after bailing. Either the time for fixed intervals of rise, or the rise for fixed intervals of time can be recorded. The first technique requires the use of chronometers, while the second, which is customary in The Netherlands, needs only a watch with a good second hand. Normally, some five readings are taken, as these will give a reliable average value for the rate of rise and also provide a check against irregularities. The time interval at which water-level readings are taken is usually from 5 to 30 seconds, depending on the hydraulic conductivity of the soil, and should correspond to a rise of about 1 cm in the water level. A good rule of thumb is that the rate of rise in mm/s in an 8 cm diameter hole with a depth of 70 cm below the watertable approximately equals the K-value of the soil in m/d.

Care should be taken to complete the measurements before 25% of the volume of water removed from the hole has been replaced by inflowing groundwater. After that, a considerable funnel-shaped watertable develops around the top of the hole. This increases resistance to the flow around and into the hole. This effect is not accounted for in the formulas or flow charts developed for the auger-hole method and consequently it should be checked that $H_o - H_t < 0.25\,(H_o - D_t)$.

After the readings have been taken, the reliability of the measurements should be checked. The difference in water level between two readings (ΔH) is therefore computed to see whether the consecutive readings are reasonably consistent and whether the value of ΔH gradually decreases.

It often happens that ΔH is relatively large for the first reading, because of water dripping along the walls of the hole directly after bailing. Further inconsistencies in ΔH values may be caused by the float sticking to the wall or by the wind blowing the tape against the wall. Consistency can be improved by tapping the tape regularly. An example of recorded data and the ensuing calculations is presented in Table 12.4.

The auger-hole method measures the K-value mainly around the hole. It gives no information about vertical K-values nor about K-values in deeper soil layers. The method is therefore more useful in shallow than in deep aquifers.

12.6.2 Inversed Auger-Hole Method

Principles and Theory of the Infiltration Process

If one uses a steel cylinder (also called 'infiltrometer') to infiltrate water continuously into unsaturated soil, one will find after a certain time that the soil around and below the area becomes almost saturated and that the wetting front is a rather sharp boundary between wet and dry soil (Figure 12.15).

We shall consider a point just above the wetting front at a distance z below the soil surface in the area where the water infiltrates. The matric head of the soil at this point has a (small) value h_m. The head at the soil surface equals $z + h$ (h = height of water level in the cylinder). The head difference between the point at depth z and a point at the soil surface equals $z + h + |h_m|$, and the average hydraulic gradient between the two points is

$$s = \frac{z + h + |h_m|}{z} \qquad (12.13)$$

Table 12.4 Example of measurements and calculations with the auger-hole method

No:	Date:	
Location:	Details:	
Depth of auger-hole D'	: 240 cm below reference	
Depth of watertable D_1	: 114 cm below reference	
$D_2 = D' - D_1$	: 126 cm	
Auger-hole radius r	: 4 cm	
Depth impermeable layer	: $D > 1/4\ D_2$	
t (s)	H (cm)	$\Delta H^{*)}$ (cm)
0	145.2	-
10	144.0	1.2
20	142.8	1.2
30	141.7	1.1
40	140.6	1.1
50	139.6	1.0

Try t = 50 s; $\Delta H_{50} = H_0 - H_{50} = 145.2 - 139.6 = 5.6$ cm

Check $H_0 - H_{50} < 0.25\ (H_0 - D_1)$; $145.2 - 139.6 < 0.25\ (145.2 - 114)$; $5.6 < 7.8$ O.K.**)

Equation 12.12: $h' = 0.5\ (145.2 + 139.6) - 114 = 28.4$ cm

Ratio's for Equation 12.10: $D_2/r = 31.5$; $h'/D_2 = 0.225$; $r/h' = 0.141$

Equation 12.10: $$C = \frac{4000 \times 0.141}{(20 + 31.5)(2 - 0.255)} = 6.2$$

Equation 12.9: $K = 6.2 \times 5.6 / 50 = 0.7$ m/d

*) per reading; $\Delta H = H_{t-1} - H_t$
**) if not O.K., try t = 40 s or less, so that ΔH_t decreases

If z is large enough, s approximates unity. Hence, from Darcy's Law (Equation 12.2), we know that the mean flow velocity in the wetted soil below approaches the hydraulic conductivity (v = K), assuming the wetted soil is practically saturated.

The inversed auger-hole method (in French literature known as the 'Porchet method') is based on these principles. If one bores a hole into the soil and fills this hole with water until the soil below and around the hole is practically saturated, the infiltration rate v will become more or less constant. The total infiltration Q will then be equal to $v \times A$ (where A is the surface area of infiltration). With v = K, we get: $Q = K \times A$.

For the inversed auger-hole method, infiltration occurs both through the bottom and the side walls of the hole (Figure 12.16). Hence we have $A = \pi r^2 + 2\pi rh$ (where r is the radius of the hole and h is the height of the water column in the hole). So we can write $Q = 2\pi Kr(h + \frac{1}{2} r)$.

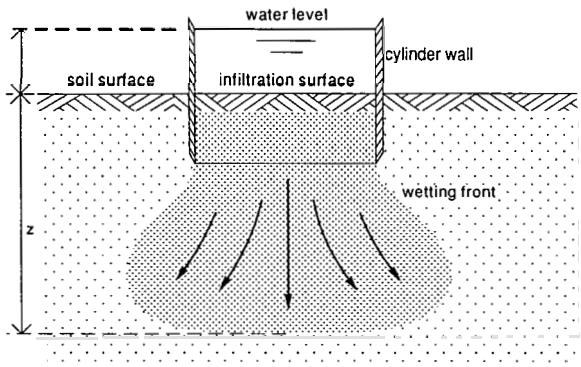

Figure 12.15 Infiltration process beneath a cylinder infiltrometer

Further, we can find Q from the rate at which the water level in the hole is lowered: $Q = -\pi r^2 dh/dt$. Eliminating Q in both expressions gives $2K(h + \frac{1}{2} r) = -r\ dh/dt$. Upon integration and rearrangement, we obtain

$$K = 1.15\, r \frac{\log(h_0 + \frac{1}{2} r) - \log(h_t + \frac{1}{2} r)}{t - t_0} \qquad (12.14)$$

where (Figure 12.17)

t = time since the start of measuring (s)
h_t = the height of the water column in the hole at time t (cm)
h_o = h_t at time t = 0

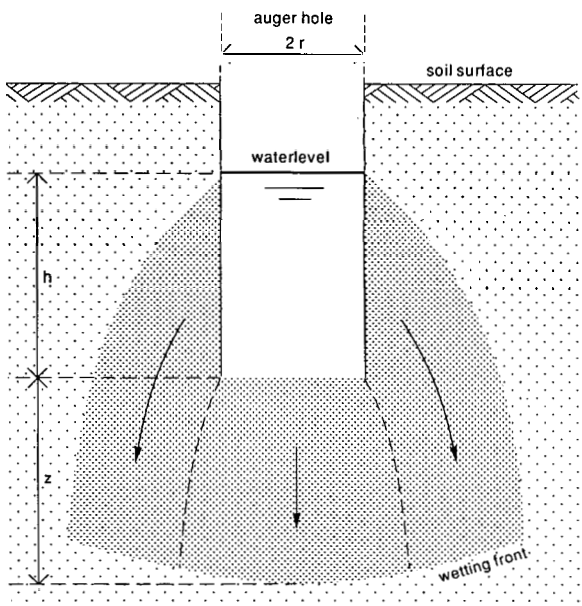

Figure 12.16 Infiltration from a water-filled auger-hole into the soil (inversed auger-hole method)

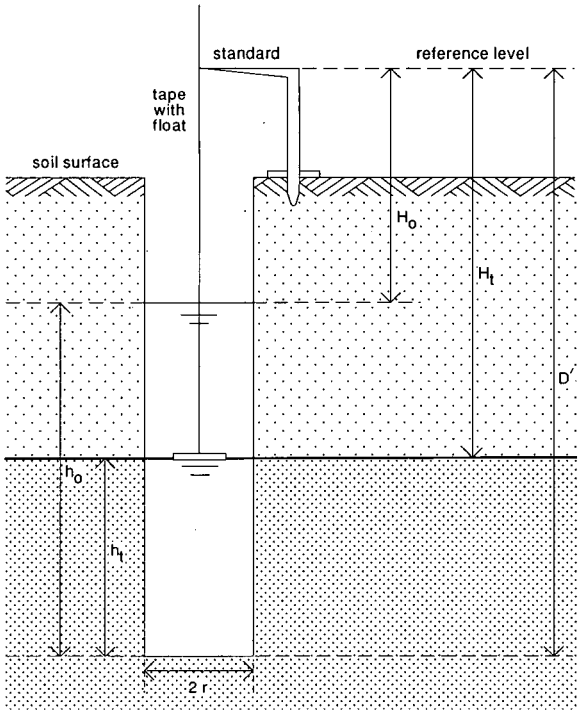

Figure 12.17 Measurements for the inversed auger-hole method

The values of h_t are obtained from

$$h_t = D' - H_t \tag{12.15}$$

where

D' = the depth of the hole below reference level (cm)
H_t = the depth of the water level in the hole below reference level (cm)

When H and t are measured at appropriate intervals (as was explained in the previous section), K can be calculated.

On semilog paper, plotting $h_t + \frac{1}{2}r$ on the log axis and t on the linear axis produces a straight line with a slope

$$\tan \alpha = \frac{\log(h_0 + \frac{1}{2} r) - \log(h_t + \frac{1}{2} r)}{t - t_0} \tag{12.16}$$

The calculation of K with Equation 12.14 can therefore also be done with the value of $\tan \alpha$. Hence, $K = 1.15\, r \tan \alpha$.

Procedure

After a hole is augered in the soil to the required depth, the hole is filled with water, which is left to drain away freely. The hole is refilled with water several times until the soil around the hole is saturated over a considerable distance and the infiltration (rate) has attained a more or less constant value. After the last refilling of the hole,

Table 12.5 Example of measurements with inversed auger-hole method (r = 4 cm, D′ = 90 cm)

t (s)	H_t (cm)	$h_t = D' - H_t$ (cm)	$h_t + \frac{1}{2}r$ (cm)
0	71	19	21
140	72	18	20
300	73	17	19
500	74	16	18
650	75	15	17
900	76	14	16

the rate of drop of the water level in the hole is measured (e.g. with the float and tape system as was explained for the auger-hole method). The data ($h + \frac{1}{2}r$ and t) are then plotted on semi-log paper, as was explained earlier. The graph should yield a straight line. If the line is curved, continue to wet the soil until the graph shows the straight line. Now, with any two pairs of values of $h + \frac{1}{2}r$ and t, the K value can be calculated according to Equation 12.14. An example of measurements is given in Table 12.5.

The data of Table 12.5 are plotted in Figure 12.18, which shows that a linear relation exists between $\log(h_t + \frac{1}{2}r)$ and t. The K-value can now be calculated from Equation 12.14 as follows

$$t_0 = 140 \quad h_0 + \tfrac{1}{2}r = 20 \quad \log(h_0 + \tfrac{1}{2}r) = 1.30$$
$$t = 650 \quad h_t + \tfrac{1}{2}r = 17 \quad \log(h_t + \tfrac{1}{2}r) = 1.23$$

$$K = 1.15 \times 4 \frac{1.30 - 1.23}{650 - 140} = 0.00063 \text{ cm/s or } 0.55 \text{ m/d}$$

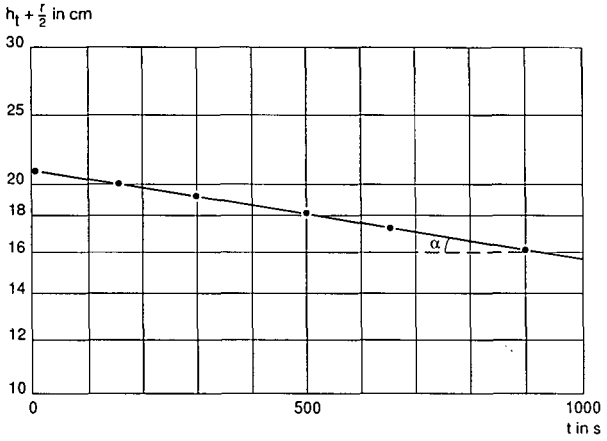

Figure 12.18 Fall of the water level, recorded with the inversed auger-hole method, plotted against time

12.7 Examples of Methods Using Parallel Drains

12.7.1 Introduction

When one is analyzing the relationships between hydraulic head (elevation of the watertable) and the discharge of pipe drainage systems to assess the soil's hydraulic conductivity, one needs a drainage equation in agreement with the conditions during which the measurements were made. Usually, the measurements are made during a dry period following a period of recharge by rain or irrigation (i.e. during tail recession). Hence, the watertable is falling after it had risen as a result of the recharge. Under such unsteady-state conditions, Equation 8.36 (Chapter 8) is applicable for ideal drains (i.e. drains without entrance resistance)

$$q = \frac{2\pi K_b d h}{L^2}$$

which can be extended to include the flow above the drain level (Oosterbaan et al. 1989)

$$q = \frac{2\pi K_b d h + \pi K_a h^2}{L^2} \qquad (12.17)$$

where

- q = drain discharge (m/d)
- K_b = hydraulic conductivity of the soil below drain level (m/d)
- K_a = hydraulic conductivity of the soil above drain level (m/d)
- d = Hooghoudt's equivalent depth (m)
- h = elevation of the watertable midway between the drains relative to drain level (m)
- L = drain spacing (m)

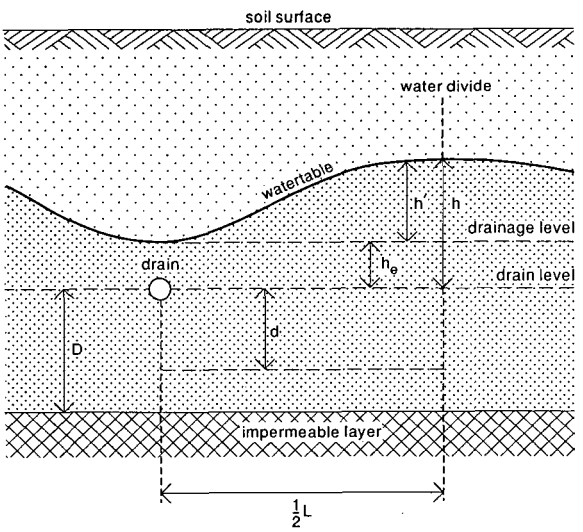

Figure 12.19 Drains with entrance resistance (symbols as defined for Equations 12.17 – 12.19)

Since entrance resistance is not always negligible, Oosterbaan et al. (1989) showed that Equation 12.17 can be adjusted to take the entrance head into account (Figure 12.19)

$$q = \frac{2\pi K_b (h - h_e) + \pi K_a (h - h_e)(h + h_e)}{L^2} \tag{12.18}$$

or

$$q = \frac{2\pi K_b d h' + \pi K_a h' h^*}{L^2} \tag{12.19}$$

where, in addition to the previously defined symbols

h_e = entrance head (i.e. the elevation of the watertable above the drains relative to drain level) (m)

h' = $h - h_e$; available hydraulic head (i.e. the elevation of the watertable midway between the drains relative to drainage level) (m)

$h^* = h + h_e$ (m)

The equivalent depth d, which is a function of the depth to the impermeable layer D, the drain spacing L, and the drain radius r_o, can be determined according to the flow chart in Figure 8.4 (Chapter 8), and the wet perimeter, u, can be chosen according to Section 8.2.2. In theory, the d-value must be calculated with an adjusted radius $r' = r_o + h_e$ instead of r_o, and the factor 8 must be replaced by 2π, but neglecting this does not usually lead to any appreciable error in the K-values.

The procedures discussed in the following sections are based on Equations 12.18 and 12.19. Statistical methods (Chapter 6, Section 6.5.4) are used to account for random variations.

12.7.2 Procedures of Analysis

To determine the K-value in an area with existing drains, one observes the depth of the watertable midway between the drains, and near the drains, and converts the measurements to hydraulic-head and entrance-head values, respectively. Observations should be made in one or more cross-sections over the drains, at different times during periods of tail recession. The drain discharge is measured at the same time. The measured discharge in m^3/d should be expressed per unit surface area of the zone of influence of the drain (i.e. the drain length multiplied by the drain spacing), obtaining q in m/d.

Equation 12.19 may also be written as

$$\frac{q}{h'} = a h^* + b \tag{12.20}$$

with

$$a = \frac{\pi K_a}{L^2} \quad \text{and} \quad b = \frac{2\pi K_b d}{L^2}$$

Plotting the values of q/h' on the vertical axis against the values of h^* on the horizontal

axis in a graph may result in one of the different lines depicted in Figure 12.20. According to the type of line, one follows different procedures, as will be explained below.

Procedure 1

Procedure 1 is used if q/h′ plotted against h* yields a horizontal line (Type I in Figure 12.20). The value of a (Equation 12.20) is close to zero, so the flow above drain level can be neglected. Consequently, the hydraulic resistance is mainly due to flow below drain level. For each set of (q, h, h_e) data, and the equivalent depth, d, from Chapter 8, we calculate the hydraulic conductivity, K_b, using Equation 12.20 with a = 0

$$K_b = \frac{L^2}{2\pi d}\frac{q}{h'} = \frac{L^2}{2\pi d}b \qquad (12.21)$$

We then determine the mean value of K_b, its standard deviation, and the standard error of the mean. We find the upper and lower confidence limits of K_b, using Student's t-distribution, as was explained in Chapter 6, Section 6.5.2. Procedure 1 will be used in Example 12.3 (Section 12.7.3).

Procedure 2

Procedure 2 is used if q/h′ plotted against h* yields a straight line of Type II (Figure 12.20). The slope of the line, a, (Equation 12.20) represents the value of the hydraulic conductivity above drain level. The line passes through the origin; the zero intercept points towards a negligible flow below drain level. These drains are resting on an impermeable layer. With each set of (q, h, h_e) data, we calculate the K_a-value, using Equation 12.20 with b = 0

$$K_a = \frac{L^2}{\pi h^*}\frac{q}{h'} = \frac{L^2}{\pi}a \qquad (12.22)$$

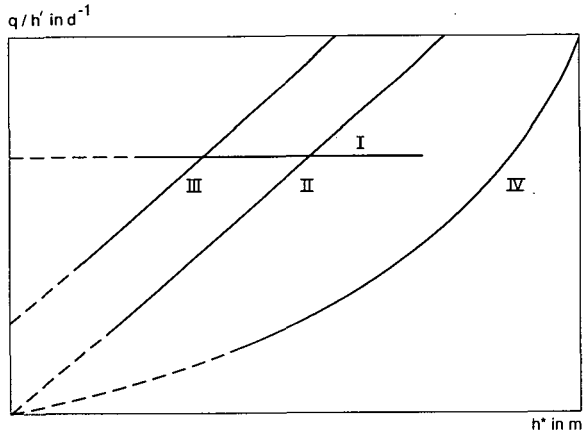

plot of q / h′ versus h*, (h = h - h_e/ h* = h + h_e)

Figure 12.20 Different patterns in plotted field data on drain discharge and hydraulic head; I) No horizontal flow above drain level; II) No horizontal flow below drain level; III) Horizontal flow occurs above and below drain level; IV) Similar to pattern II, but with a high entrance head and/or decreasing K_a value with deph

We then determine the mean and standard error of K_a, and the standard error of the mean. With Student's t-distribution, we find confidence limits of K_a and of $\bar{K}_a$ (Section 6.5.2). Procedure 2 will be used in Example 12.4 (Section 12.7.4).

Procedure 3

Procedure 3 is used if q/h′ plotted against h* yields a straight line that does not pass through the origin (Type III in Figure 12.20). In this case, there is flow above and below the drain level, and neither K_a nor K_b can be neglected. We then perform a linear two-way regression analysis with the equations

$$\frac{q}{h'} = a\,h^* + b \tag{12.23}$$

and

$$h^* = a'\frac{q}{h'} + b' \tag{12.24}$$

Writing Equation 12.24 in the same form as Equation 12.23 gives

$$\frac{q}{h'} = \frac{h^*}{a'} - \frac{b'}{a'} \tag{12.25}$$

We thus find two different regression coefficients, a and 1/a′, which we can combine into an intermediate regression coefficient, a*, by taking their geometric mean. Also, we find an intermediate value b* (Chapter 6, Section 6.5.4). Using Equation 12.20, we can find the K_a and K_b values from the intermediate values a* and b* instead of a and b. Following Chapter 6, the confidence limits of K_a and K_b are found from the confidence limits of a* and b*. The width of the confidence intervals will be somewhat underestimated, because the variables q/h′ and h* are not fully independent since both h′ and h* contain parameters h and h_e.

Often, a simpler procedure for finding the confidence limits can be used, because the values a (from Equation 12.23) and 1/a′ (from Equation 12.25) give a reasonable approximation of the confidence limits of a*. Similarly, we find the approximate confidence limits of b* as b and b′/a′. Example 12.5 will use Procedure 3, including these approximations of the confidence intervals.

Procedure 4

Procedure 4 is used if q/h′ plotted against h* yields an upward-bending curve which passes through the origin (Type IV in Figure 12.20). In this case, there is no flow below drain level and K_b can be neglected. The K_a-value is not constant, but decreases with depth. We write $K_a = \lambda\,h^*$, so that substitution into Equation 12.19 with $K_b = 0$ yields

$$\frac{q}{h'} = \frac{\pi\lambda h^{*2}}{L^2} \tag{12.26}$$

Now, a plot of q/h′ versus h^{*2} may yield a straight line going through the origin (Figure 12.21). Next, for each set of (q, h, h_e) data, we calculate the λ-value. We then determine its mean, $\bar{\lambda}$, and standard deviations of λ and $\bar{\lambda}$. With Student's t-distribution, we can find the confidence limits of λ and $\bar{\lambda}$. An example of this procedure was given by Oosterbaan et al. (1989).

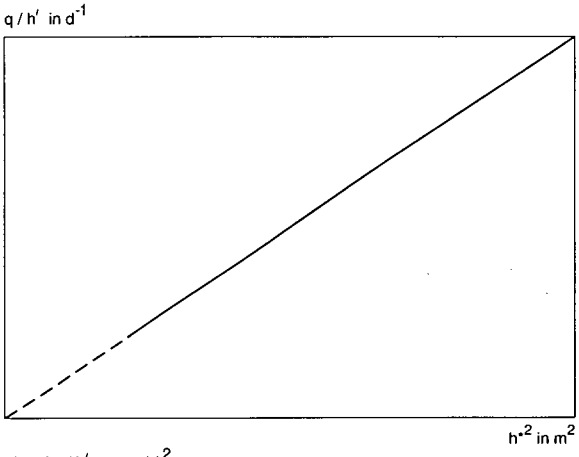

plot of q / h' versus h*2

Figure 12.21 Plot of field data used in Procedure 4

Table 12.6 Field observations on drain discharge and hydraulic head (Example 12.3)

No.	q (m/d)	h (m)	h_e (m)	h' (m)	K_b (m/d)
1	0.0030	0.31	0.01	0.30	0.34
2	0.0040	0.40	0.05	0.35	0.39
3	0.0030	0.50	0.10	0.40	0.25
4	0.0045	0.50	0.05	0.45	0.34
5	0.0060	0.70	0.20	0.50	0.40
6	0.0050	0.60	0.10	0.50	0.34
7	0.0040	0.55	0.05	0.50	0.27
8	0.0050	0.63	0.08	0.55	0.31
9	0.0045	0.72	0.12	0.60	0.25
10	0.0070	0.70	0.10	0.60	0.39
11	0.0060	0.80	0.20	0.60	0.34
12	0.0045	0.75	0.15	0.60	0.25
13	0.0040	0.85	0.25	0.60	0.22
14	0.0050	0.70	0.05	0.65	0.26
15	0.0045	0.75	0.10	0.65	0.23
16	0.0050	0.85	0.15	0.70	0.24
17	0.0060	0.95	0.20	0.75	0.27
18	0.0050	0.90	0.15	0.75	0.22

12.7.3 Drains with Entrance Resistance, Deep Soil

Example 12.3

Table 12.6 shows the data collected on drain discharge, hydraulic head midway between the drains, and entrance head (q, h, and h_e) in an experimental field with drain spacing L = 20 m and a drain radius r_o = 0.1 m. The impermeable layer is at great depth.

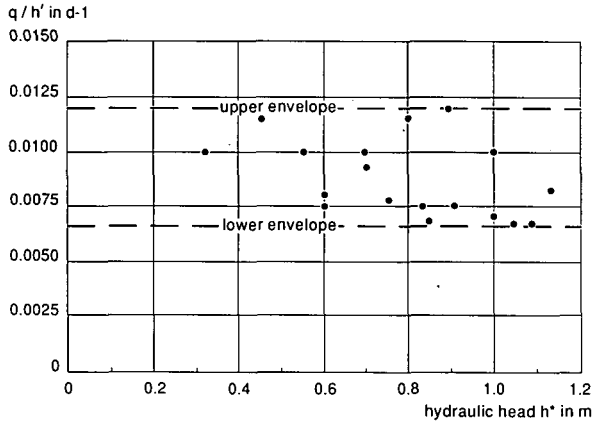

Figure 12.22 Plot of field data indicating a negligible flow resistance above drain level (Example 12.3)

A plot of q/h′ versus h* values (Figure 12.22) shows that the envelope lines tend to be horizontal, indicating that resistance to flow above drain level can be neglected. Hence, Procedure 1 and Equation 12.21 are applicable. According to Table 8.1 (Chapter 8), Hooghoudt's equivalent depth d = 1.89 m. The K_b-values thus found are shown in Table 12.6.

The K_b-values in Table 12.6 have a mean value $\bar{K}_b = 0.30$ m/d. The standard error of the mean is 0.014 m/d. Using Student's probability distribution (Section 6.5.2) for a 90% confidence interval and 17 degrees of freedom ($t_f = 1.75$), we can state with 90% confidence that

$$0.28 < \bar{K}_b < 0.32 \text{ m/d}$$

12.7.4 Drains with Entrance Resistance, Shallow Soil

Example 12.4

Table 12.7 shows the data collected in experimental fields in the delta of the Tagus River in Portugal, in which corrugated and perforated PVC pipe drains with a radius $r_o = 0.10$ m were installed at a depth of 1.1 m below the soil surface and at a spacing L = 20 m. The soils in this delta are fine textured (heavy clay soil).

Figure 12.23A shows the drainage intensity, q/h′, plotted against the h*-values of Table 12.7. The relation between q/h′ and h* shows an upward-bending curve through the origin of the graph. This suggests that the soil below drain level is impermeable and that the soil above drain level has a K-value that decreases with depth. If we ignore the two highest points in Figure 12.23A, however, we can make the assumption that the relationship between q/h′ and h* gives a straight line through the origin of the graph or, in other words, that the soil above drain level has a constant K-value, whereas the flow below the drains is neglected. This assumption is illustrated by the straight line in Figure 12.23A.

Hence, Procedure 2 is used and the hydraulic conductivity K_a is calculated according to Equation 12.22. Table 12.7 shows the results. The mean $\bar{K}_a$ equals 0.20 m/d. The

Table 12.7 Field observations on drain discharge and hydraulic head (Example 12.4)

No.	Date	q (m/d)	h (m)	h_e (m)	h′ (m)	h^* (m)	q/h′ (d^{-1})	K_a (m/d)
1	29/12	0.00137	0.88	0.18	0.70	1.06	0.00196	0.235
2	30/12	0.00106	0.85	0.13	0.72	0.98	0.00147	0.191
3	31/12	0.00064	0.73	0.08	0.65	0.81	0.00098	0.155
4	02/01	0.00030	0.61	0.03	0.58	0.64	0.00052	0.103
5	03/01	0.00026	0.58	0.02	0.56	0.60	0.00046	0.099
6	07/01	0.00129	0.82	0.16	0.66	0.98	0.00195	0.254
7	08/01	0.00124	0.84	0.18	0.66	1.02	0.00188	0.235
8	09/01	0.00126	0.82	0.12	0.70	0.94	0.00180	0.244
9	10/01	0.00084	0.77	0.10	0.67	0.87	0.00125	0.183
10	13/01	0.00035	0.50	0.01	0.49	0.51	0.00071	0.178
11	21/02	0.00303	0.98	0.54	0.44	1.52	0.00689	0.577
12	22/02	0.00263	0.96	0.45	0.51	1.41	0.00516	0.466
13	25/02	0.00129	0.91	0.20	0.71	1.11	0.00182	0.208
14	26/02	0.00086	0.88	0.18	0.70	1.06	0.00123	0.148
15	28/02	0.00043	0.73	0.01	0.72	0.74	0.00060	0.103
16	03/03	0.00027	0.53	0.00	0.53	0.53	0.00051	0.122
17	05/03	0.00040	0.69	0.02	0.67	0.71	0.00060	0.107
18	06/03	0.00031	0.61	0.01	0.60	0.62	0.00052	0.106
19	07/03	0.00026	0.60	0.00	0.60	0.60	0.00043	0.092

standard deviation of K_a equals 0.13 m/d and the standard error of $\bar{K}_a$ equals 0.032 m/d. We can calculate the confidence interval of the mean $\bar{K}_a$ using Student's t-distribution (Section 6.5.2). With 90% confidence and 16 degrees of freedom (Observations 11 and 12 are omitted), we find it to range from 0.14 to 0.26 m/d.

Discussion

As stated earlier, the procedure for the calculation can be improved by accepting that the value of K_a decreases with depth, as occurs frequently in heavy clay soils. This is also suggested in Table 12.7, by the decrease in the K_a-values with decreasing q- and h-values. Oosterbaan et al. (1989) calculated that the K_a-value is 0.77 m/d at the soil surface, 0.22 m/d at 0.55 m depth, and almost zero at drain level. From this analysis, it follows that the drains are situated in a slowly permeable soil layer, which explains the presence of the entrance resistance. It is likely that the entrance head would have been less if the drains had been placed less deeply. In soils like those found in the experimental plot, the optimum drain depth is probably about 0.8 m.

Figure 12.23B, which shows a plot of q against h_e, indicates that the entrance head increases proportionally with the discharge. This corresponds to the previous conclusion that the K_a-value is small at drain depth.

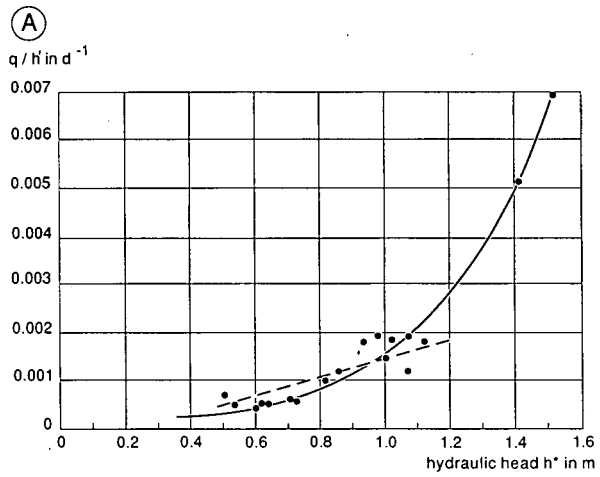

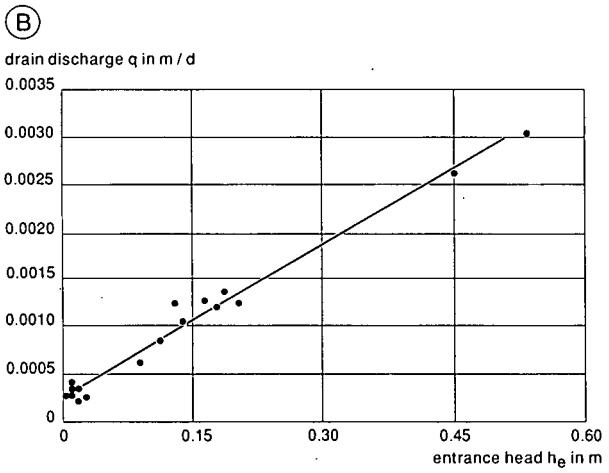

Figure 12.23 Plots of field data from the Leziria Grande (Example 12.4)
A: The hydraulic conductivity above the drains decreases with depth
B: Plot of drain discharge against entrance head

12.7.5 Ideal Drains, Medium Soil Depth

Example 12.5

Table 12.8 shows data on h and q in an experimental field with drain spacing L = 20 m and drain radius r_o = 0.1 m. The entrance resistance was assumed to be negligibly small, so the h_e-values were not measured. Hence, the drains are supposed to function as ideal drains and $h_e = 0$. Note that $h' = h^* = h$.

A plot of q/h versus h-values (Figure 12.24) suggests that the relationship between these two parameters is an upward-sloping straight line that does not pass through the origin, indicating that the flow to the drains occurs above and below the drain

Table 12.8 Data on drain discharge and available hydraulic head used in Example 12.5

No.	q (m/d)	h (m)	q/h (d^{-1})
1	0.00125	0.16	0.00781
2	0.00099	0.17	0.00582
3	0.00137	0.18	0.00761
4	0.00132	0.20	0.00660
5	0.00274	0.28	0.00979
6	0.00342	0.32	0.01069
7	0.00316	0.34	0.00929
8	0.00483	0.35	0.01380
9	0.00414	0.38	0.01089
10	0.00342	0.38	0.00900
11	0.00570	0.41	0.01390
12	0.00482	0.43	0.01121

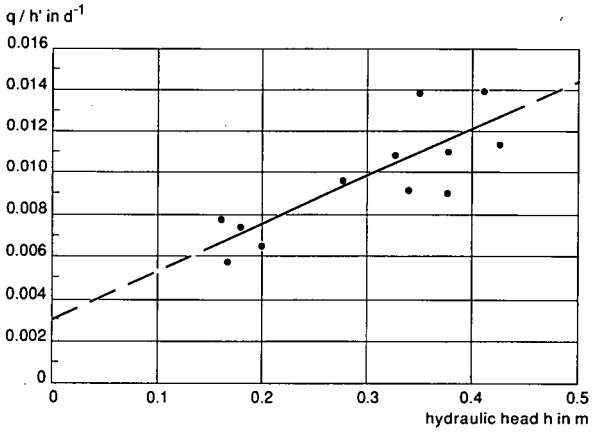

Figure 12.24 Plot of field data indicating flow above and below the drain level (Example 12.5)

level. Procedure 3 can therefore be applied, and a regression analysis is made.

Applying the principles explained in Section 12.7.3 and using Equations 12.23 to 12.25, we find

a) Regression of q/h upon h

$$\frac{q}{h} = 0.021\ h + 0.0035$$

b) Regression of h upon q/h

$$h = 30.9\frac{q}{h} - 0.0058$$

or

$$\frac{q}{h} = 0.032\,h - 0.000019$$

The calculation of the K-values proceeds as follows. Using Equation 12.20, a = 0.021 yields K_a = 2.6 m/d, and 1/a′ = 0.032 yields K_a = 4.1 m/d. Using these values as the approximate confidence limits, we find that $2.6 < K_a < 4.1$ m/d. Similarly, b = 0.0035 yields $K_bd = 0.22\ m^2/d$, and b′/a′ = –0.000019 yields $K_bd = -0.0012\ m^2/d$.

A comparison of the K_a- and K_bd-values shows that the K_a-value is the dominating one, and that the K_bd-value is statistically insignificant. Note that if we assume that the flow below drain level can be neglected, we can use Procedure 2 to analyze the data of Example 12.5 as well. This would give $\bar{K}_a$ = 4.3 m/d, with a standard error of the mean of 0.26 m/d.

References

Abrol, I.P., J.S.P. Yadav, and F.I. Massoud 1988. Salt-affected soils and their management. FAO Soils Bulletin 39, Rome, 131 p.

Amer, M.H. and N.A. de Ridder 1989. Land drainage in Egypt. DRI, Cairo. 377 p.

Anderson, S.H., and D.K. Cassel 1986. Statistical and autoregressive analysis of soil physical properties of Portsmouth sandy loam. Soil Science Society of American Journal 50, pp. 1096-1104.

Aronovici, V.S. 1947. The mechanical analysis as an index of subsoil permeability. Soil Science Society of American Proc. 11, pp. 137-141.

Ayers, R.S., and D.W. Westcott 1985. Water quality for agriculture. Rev. ed. Irrigation and Drainage Paper 29, FAO, Rome, 174 p.

Bentley, W.J., R.W.Skaggs, and J.E. Parsons 1989. The effect of variation in hydraulic conductivity on watertable drawdown. Technical Bulletin, North Carolina Agricultural Research Service, North Carolina State University, 288, Raleigh, 23 p.

Bouma, J., A. Jongerius, and D. Schoonderbeek 1979. Calculation of saturated hydraulic conductivity of some pedal clay soils using micromorphometric data. Soil Science Society of American Journal 43, pp. 261-264.

Bouma, J., J.W. van Hoorn, and G.H. Stoffelsen 1981. Measuring the hydraulic conductivity of soil adjacent to tile drains in a heavy clay soil in The Netherlands. Journal of Hydrology 50, pp. 371-381.

Boumans, J.H. 1976. Drainage calculations in stratified soils using the anisotropic soil model to simulate hydraulic conductivity conditions. In: J. Wesseling (ed.), Proceedings of the international drainage workshop. ILRI Publication 25, Wageningen, pp. 108-123.

Bouwer, H., and R.D. Jackson 1974. Determining soil properties. In: J. van Schilfgaarde (ed.), Drainage for Agriculture. Agronomy 17. American Society of Agronomy, Madison, pp. 611-672.

Camp, C.R. 1977. Determination of hydraulic conductivity for a Louisiana alluvial soil. Third National Drainage Symposium Proceedings. American Society Agricultural Engineers, Michigan, pp. 1-77.

Childs, E.C. 1943. The watertable, equipotentials and streamlines in drained land. Soil Science 56, pp. 317-330.

De Ridder, N.A. and K.E. Wit 1965. A comparative study on the hydraulic conductivity of unconsolidated sediments. Journal of Hydrology 3, pp. 180-206.

Dieleman, P.J., and B.D. Trafford 1976. Drainage testing. Irrigation and Drainage Paper 28, FAO, Rome, 172 p.

El-Mowelhi, N.M., and J. van Schilfgaarde 1982. Computation of soil hydrological constants from field drainage experiments in some soils in Egypt. Transaction of the American Society Agricultural Engineers, pp. 77-79.

Kuntze, H. 1964. Einflusz der Dränung auf die Struktur des Marsch Bodens. Zeitschrift für Kulturtechnik und Flurbereinigung 5 (3), pp. 129-134.

Marshall, T.J. 1957. Permeability and the size distribution of pores. Nature 180, pp. 664-665.

Oosterbaan, R.J., A. Pissarra, and J.G. van Alphen 1989. Hydraulic head and discharge relations of pipe drainage systems with entrance resistance. Proceedings 15th European Regional Conference on Agricultural Water Management. Vol. III. ICID, Dubrovnik, pp. 86-98.

Oosterbaan, R.J. 1990a. Single pipe drains with entrance resistance above a semi-confined aquifer. In: Symposium on Land Drainage for Salinity Control, Vol. 3. Cairo, pp. 36-46.

Oosterbaan, R.J. 1990b. Parallel pipe drains with entrance resistance above a semi-confined aquifer with upward seepage. In: Symposium on Land Drainage for Salinity Control, Vol. 3. Cairo, pp. 26-35.

Oosterbaan, R.J. and H.P. Ritzema 1992. Hooghoudt's drainage equation, adjusted for entrance resistance and sloping land. In: W.F. Vlotman (ed.), Proceedings 5th International Drainage Workshop, Vol. II. ICID/WAPDA, Lahore, pp. 2.18-2.28.

Reynolds, W.D., and D.E. Elrick 1985. In-situ measurement of field saturated hydraulic conductivity, sorptivity, and the a-parameter, using the Guelph permeameter. Soil Science, 140, 4, pp. 292-302.

Richards, L.A. (ed.) 1954. Diagnosis and improvement of saline and alkaline soils. Agriculture Handbook 60. USDA, Washington, 160 p.

Scheltema, W. and H.Ch.P.M. Boons 1973. Al-clay, a solution to mechanical stability problems in a heavy clay soil? In: H. Dost (ed.), Acid sulphate soils : proceedings of the international symposium on acid sulphate soils. Vol. II. ILRI Publication 18, Wageningen, pp. 319-342.

Smedema, L.K., and D.W. Rycroft 1983. Land drainage : planning and design of Agricultural Drainage Systems. Batsford, London, 376 p.

Van Beers, W.F.J. 1970. The auger-hole method : a field measurement of the hydraulic conductivity of soil below the watertable. Rev. ed. ILRI Bulletin 1, Wageningen, 32 p.

Van Hoorn, J.W. 1958. Results of a groundwater level experimental field with arable crops on a clay soil. Netherlands Journal Agricicultural Science, 6, pp. 1-10.

Wit, K.E. 1967. Apparatus for measuring hydraulic conductivity of undisturbed soil samples. Technical Bulletin 52. Institute for Land and Water Management Research, Wageningen, 12 p.

Wösten, J.H.M. 1990. Use of soil survey data to improve simulation of water movement in soils. Thesis, Agricultural University, Wageningen, 103 p.

Zangar, C.N. 1953. Theory and problems of water percolation. U.S. Bureau of Reclamation. Engineering Monograph No. 8, Denver, 76 p.